IOP Publishing European Journal of Physics
Eur. J. Phys. **41** (2020) 025201 (12pp) https://doi.org/10.1088/1361-6404/ab5e77

Computational relaxation method for modeling electrostatic systems with non-trivial geometries

Felipe Reyes-Osorio, Juan Manuel Scarpetta-Ramirez and Karen Rodriguez-Ramirez

Departamento de Física, Universidad del Valle, A.A 25360, Cali, Colombia

E-mail: reyes.felipe@correounivalle.edu.co, scarpetta.juan@correounivalle.edu.co and karem.c.rodriguez@correounivalle.edu.co

Received 5 August 2019, revised 5 November 2019
Accepted for publication 3 December 2019
Published 12 February 2020

Abstract

Through electrostatic potential, it is possible to analyze an electromagnetic system and find the generated electric field and charge distribution for a given setup. However, most boundary conditions prove to be impossible to solve analytically. In the following paper, we present a computational relaxation method for modeling the potential, electric field and charge density of 2D electromagnetic systems with non-trivial geometries. By performing the experimental realization of finite parallel plates, we find an astonishing agreement between experimental results and our model. We study the uncertainties introduced by the model by comparing our results with theoretical predictions in the specific case of infinite parallel wires, and show that the error rate drops exponentially as the system size increases. Finally, the number of iterations required to reach equilibrium has also been analyzed for different lattice-sweeping methods.

Keywords: computational methods, boundary conditions, electrostatic potential

(Some figures may appear in colour only in the online journal)

1. Introduction

The modern research landscape is such that computational methods are a crucial tool for many physicists. Although most undergraduate programs teach programming or numerical methods in some form, it can be the case that these courses forgo the application of such

methods to instead focus on the theory behind them. While a thorough theoretical understanding is of the utmost importance, a clear example and analysis will go a long way to furthering a physics student's skills.

The relaxation method is used in many sub-disciplines of physics, from fluid mechanics [1], to astrophysics [2]. Its versatility and relative simplicity make it a perfect introduction to computational methods, and its application to a familiar problem in electrostatics is sure to be illuminating for an eager learner.

Often, all the relevant information of an electrostatic system can be found from the electric potential function, which is defined as the amount of work needed to move a test charge from a reference point to another point within an electric field (section 2.2 of [3]). The electric field is therefore equal to the negative gradient of the potential.

Although it is simple, as will be shown below, to find a partial differential equation for the potential, this was not always the case. It was not until the late eighteenth and early nineteenth centuries that the scientific understanding of electricity, through the combined efforts of Coulomb, Gauss, Faraday and many other physicists, was developed [4] to the point where it was possible to reach a clear mathematical model. In particular, the introduction of the potential function by Green [5] proved to be a crucial tool in the analysis of many sub-disciplines of physics, not just electromagnetism. Later, thanks to Laplace [6], it became possible to give a mathematical formulation to this concept in the form of the eponymous equation. However, the solutions to the Laplace equation turn out to be highly dependent on the system's geometry, and often impossible to solve in terms of common functions [7]. The following paper is intended to explain and develop the computational relaxation method, and apply it to numerically solve the Laplace equation in the context of electrostatics. The content of this paper is presented in the next five sections. In section 2, we introduce the theoretical framework of the relaxation method, on which we base our approach to the electrostatic potential problem. In section 3, we show the solution provided by the developed numerical model, and in sections 4 and 5, we explore the performance of the model with respect to the computing resources it requires and the differences found when compared to the theoretical explanations. Section 6 presents the results of measuring the potential of a known configuration experimentally, which we then compare with our simulation to show its usefulness in an experimental realization. Finally, we give some closing remarks on the method and its applications in section 7.

2. Intended approach to the model

Considering the electric field as the negative gradient of the potential function, as mentioned in the previous section, and applying the differential form of Gauss' law (section 2.10 of [3]) we can retrieve the well-known Poisson equation in SI units,

$$\nabla^2\varphi = -\frac{\rho}{\varepsilon_0}, \tag{1}$$

which relates the potential φ with the local charge density ρ and the electric permittivity of free space ε_0. In the absence of charges, the equation reduces to the Laplace equation, given by

$$\nabla^2\varphi = 0. \tag{2}$$

Real-value solutions to this second-order partial differential equation are called harmonic functions. However, exact solutions to (2) in terms of known analytic functions are mathematically complicated even for simple boundary conditions. Often, this task proves to

be formidable, requiring solutions to multiple eigenvalue problems, and Fourier expansions [7]. Since conventional analytical methods turn out to be impractical for solving (2), we must turn to computational approaches.

Let us explore some properties of harmonic functions. A function f satisfies the Laplace equation if, for a spherical surface S of radius R centered at $\mathbf{r}$, it follows that [8]

$$\frac{1}{4\pi R^2}\int_S f\ da = f(\mathbf{r}), \tag{3}$$

which means that the average value of the solution over a sphere is equal to the function evaluated at its center[1].

In systems in which the conductors extend infinitely in one direction the symmetry ensures that examining a cross-section is enough to find the potential. We focus on solving this problem, so we analyze a 2D case of (2). Equation (3) changes from a sphere to a circumference [9], and since there are no constraints on R, the circle can be arbitrarily small. This suggests the following method to computationally solve the problem.

Let us divide a transverse section of the system into squared regions using a fine grid in which each lattice site has a constant potential. This space discretization must be taken into account when assigning the potential. For simplicity, we assign to the entire cell a potential equal to the value at its center. Now, the smallest possible circle around a square would include its four nearest neighboring sites, without the diagonally adjacent ones, since their centers lie outside the circumference. With a small enough grid, the lattice for the potential approximates the needed solution. From (3), we can approximate the value φ of a cell in terms of its neighbors as

$$\varphi(i,j) = \frac{1}{4}[\varphi(i+1,j) + \varphi(i-1,j) + \varphi(i,j+1) + \varphi(i,j-1)], \tag{4}$$

where i and j are the respective row and column of the evaluated position. This function is Lipschitz continuous [9], with Lipschitz constant $K = 1/4$; this means that for an arbitrary initial value of $\varphi(i,j)$, repeated applications of (4) will converge towards a valid solution. This is known as a fixed-point iteration. We now have an iterative formula to approximate our solution from an initial guess in

$$\varphi_{\text{new}}(i,j) = \frac{1}{4}[\varphi(i+1,j) + \varphi(i-1,j) + \varphi(i,j+1) + \varphi(i,j-1)]. \tag{5}$$

Equation (5) can also be retrieved with a more formal procedure [10]. Suppose an analytical function $f\colon \mathbb{R} \to \mathbb{R}$. f allows for a Taylor series decomposition, from which we retrieve a finite difference expression for the second derivative

$$\frac{\mathrm{d}^2 f(x)}{\mathrm{d}x^2} = \frac{f(x+h) + f(x-h) - 2f(x)}{h^2} + \mathcal{O}(h^2), \tag{6}$$

where $|h| \ll 1$. In the case where $f\colon \mathbb{R}^2 \to \mathbb{R}$, equation (6) allows us to find an expression for $\nabla^2 f$ in Cartesian coordinates, which we can rearrange to find

$$f(x,y) = \frac{1}{4}[f(x+h,y) + f(x-h,y) + f(x,y+h) + f(x,y-h) - h^2\nabla^2 f] + \mathcal{O}(h^4). \tag{7}$$

[1] From this it follows, by the theorem of minimum modulus, that there cannot be a stable equilibrium made by only static charges, since such a point corresponds to a minimum in the potential.

This equation directly translates to a 2D square lattice of step-size h. If f represents a potential, the term involving the Laplacian vanishes. Neglecting terms of order greater than four, and applying a fixed-point iteration, we reach the same expression [11] as (5).

In order to set boundary conditions, we can use the grid as a coordinate system to assign known values of $\varphi(i, j)$ as boundaries, and impose that they remain constant through the iterations; only lattice sites not corresponding to boundaries, known as free points, will be subject to redefinition according to (5).

Once the boundaries are set, we can run through the necessary iterations to find any particular solution. This is the relaxation method, which we use to solve the Laplace equation. We write a C/C++ program, allowing us to use large lattices, and complete more iterations.

3. Numerical solution

First, let us define three rectangular conductors at fixed potentials of 6, 12 and 18 V. The dimensions of these plates are respectively 15 × 50 m, 20 × 20 m and 18 × 10 m. This is a system with a geometry that presents a high level of difficulty for finding analytical solutions, and allows us to exemplify the relaxation method [3]. We consider these conductors hanging in the vacuum. It is important to remember that these plates would correspond to transverse sections of rectangular conducting bars of infinite length along the z-axis [12]. This configuration reduces our initial 3D problem to one of 2D, with longitudinal symmetry along the z-axis. Therefore, the complete solution to the problem is simply given by the relaxation method in the xy plane. In the free points, we set an arbitrary initial potential value; in this case they are set to 0. These free points represent the physical space between the conductors, and it is here where we desire to find the potential. After applying the relaxation method, we find that our initial guess converges towards a solution, as expected [13]. For a 100 × 100 lattice this is consistently achieved after 3000 iterations. Here, we refer to one iteration as one completed sweep of the entire grid.

The obtained data are plotted as 3D surfaces in the (a) and (b) panels of figure 1. The flat regions represent the conductors at constant potential. Note how the contour of the lattice stays at zero. This is necessary in order to keep the reference potential constant. Another way to visualize the results is by means of a density plot of the lattice, as presented in panels 1(c) and (d). One can appreciate the difference between the initial and final configuration, as well as the smoothness of the function in the equilibrium state.

From the calculated potential φ, we can evaluate the electric field **E,** since it satisfies

$$\mathbf{E} = -\vec{\nabla}\varphi = -\frac{\partial\varphi}{\partial x}\,\mathbf{i} - \frac{\partial\varphi}{\partial y}\,\mathbf{j}. \tag{8}$$

The symmetry of the system is such that the z component of the gradient vanishes. Setting the spatial steps Δx and Δy equal to the length of the sides of our cells, we can calculate the components of **E** by taking the potential difference between consecutive squares [14]. Note from (8) that we discover that **E** vanishes inside the conductors because of their constant potential. In addition, the charges in the conductors should gather at the surface, generating a charge density σ, which relates to the magnitude of the normal electric field according to

$$E = \frac{\sigma}{\varepsilon_0}. \tag{9}$$

From this, we find **E** and σ, and show the vector field plots in figure 2. We set each cell to be 1 m long, so σ and **E** are of the order of $10^{-12}\,\mathrm{C\,m^{-2}}$ and $10^{-3}\,\mathrm{V\,m^{-1}}$, respectively. These values are several orders of magnitude below those used in any practical experiment. Clearly, the side lengths and voltages should be scaled appropriately according to the situation. Our

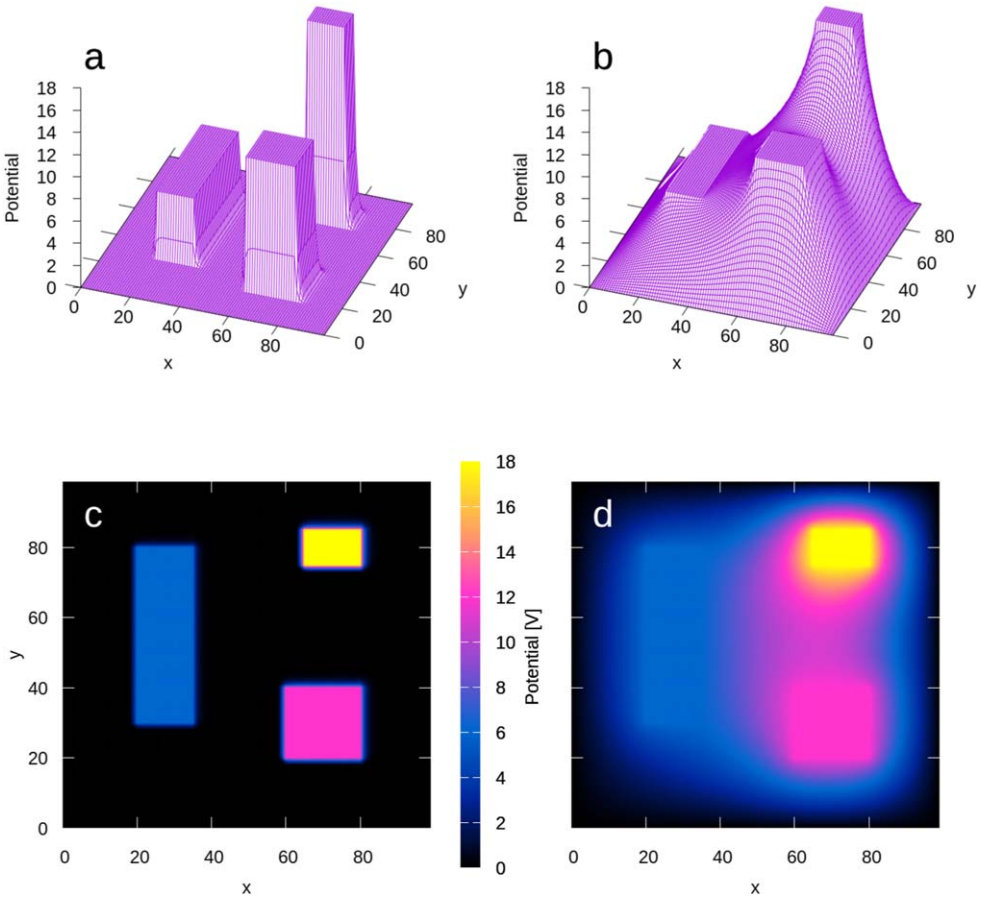

Figure 1. (a) and (c) Show the same initial boundary conditions. Raised platforms and rectangles correspond to three plates at different potentials, as referred to in this section. (b) and (d) are the potential found after running the simulation.

results also show that the charge on the conductor's surface tends to cluster in its corners, as can be clearly seen in the corners of the square geometry of panel 2(b). Furthermore, we can see that as the conductor becomes rounder, the charge distribution tends to homogenize. For instance, in figure 2(b) the corners have a charge density almost three times higher than that of the middle of the sides. This proportion diminishes as the degree of curvature increases, as shown in (c). Finally, in (d), the charge density is close to a constant over the entire border. In addition, note that the range covered by the charge densities becomes more compact as we approach a circle: from 2–16 pC m^{-2} in (b) to 1–4 pC m^{-2} in (d). Combined with the fact that the conductors on (b)–(c) are of similar size and equal potentials, we get further confirmation of the charge homogenization.

4. Convergence of the model

When applying the relaxation method we analyze two different ways of sweeping the lattice: using a systematic sampling (SS), or a random sampling (RS). The former evaluates every

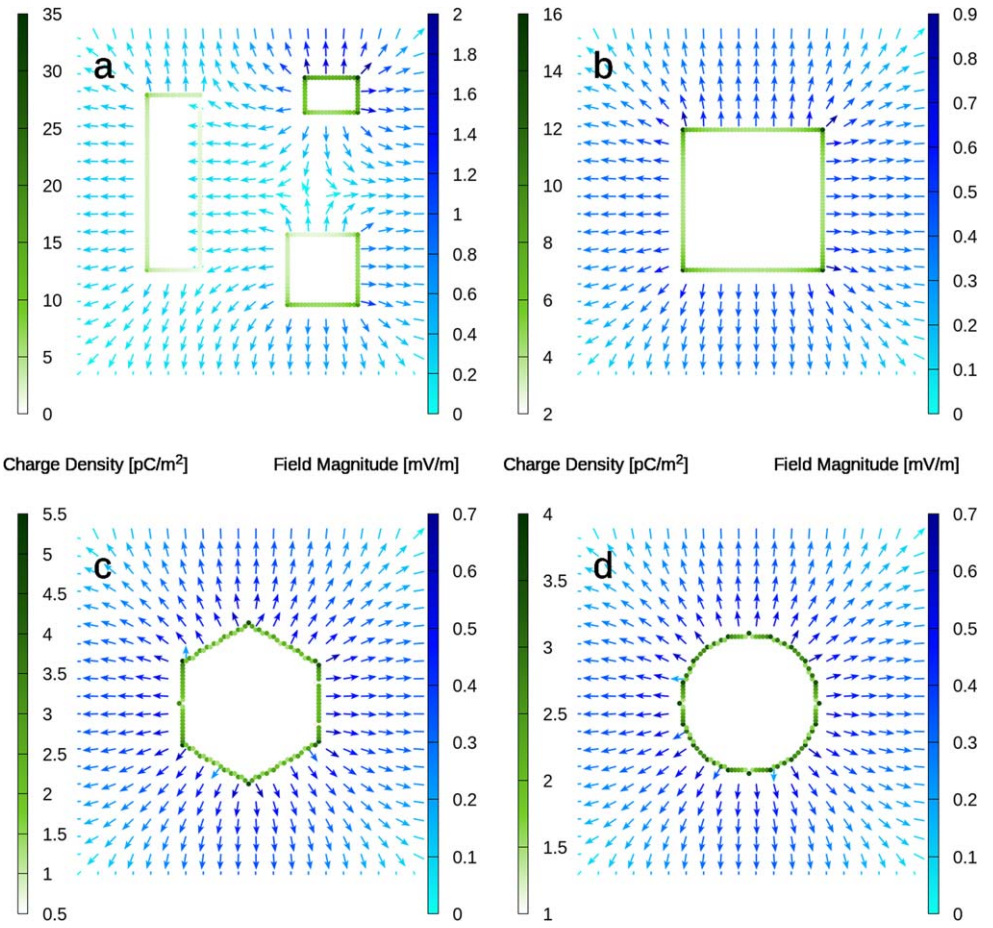

Figure 2. (a) Electric field and surface charge density for the boundary conditions from figure 1. (b)–(d) show how the charge density varies with the shape of the conductor. Clustering of charge in the corners is evident.

free space in an organized and consecutive manner, starting from the bottom left corner, advancing to the right, and resuming at the beginning of the next row to ensure a complete cover of the lattice. The latter is accomplished by randomly selecting a free point for evaluation, as done in standard Monte Carlo methods [15]. With the intention of determining which way of sweeping is better for this problem, we tracked the value of a free point near the middle of the lattice as it approached equilibrium with both methods. We used the same three-plate configuration from section 3 for both runs. The results are presented in figure 3. Recall that an iteration is a complete sweep of the lattice. In this case, we used a 100×100 lattice, meaning that an iteration entailed 10 000 evaluations. In an RS iteration, we select random free points for re-evaluation. Since the nature of RS impedes the evaluation of the entire grid consecutively, an iteration here means the re-evaluation of 10 000 random free points; this is to ensure an RS iteration is comparable to its SS counterpart. We find that, although the solutions are equivalent, SS is clearly more suitable for the relaxation method, since it takes three orders of magnitude fewer iterations than RS. Furthermore, this difference increases

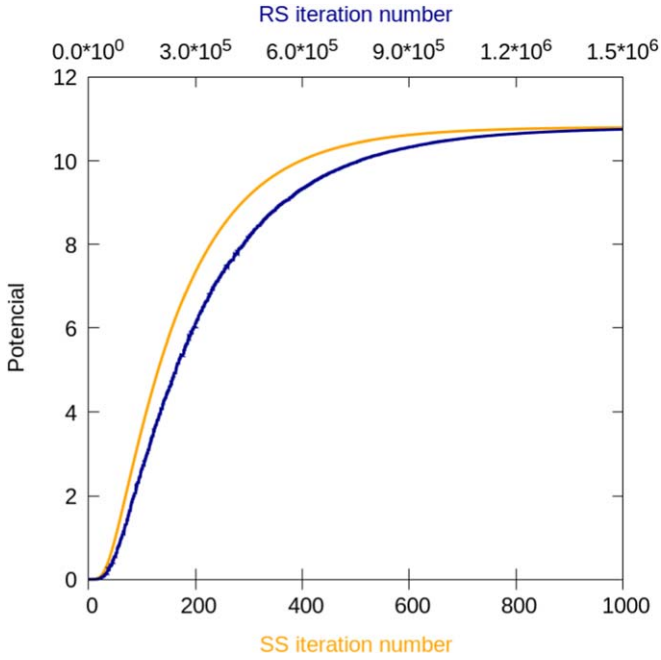

Figure 3. Comparison between the iterations required to reach equilibrium of the relaxation method using random and systematic sampling. Dark line represents the random sampling, plotted using the top x axis.

quasi-exponentially with the lattice size (a further discussion on the lattice size is presented below, in section 5).

After determining SS as the better way of sweeping, we look for further ways to optimize the numerical implementation. Our next attempt consists of changing the initial values for the free spaces. To keep things simple, we chose a new constant to replace the zero value previously used. To determine an appropriate constant, we employ two averaging procedures: in method A, we consider the average of the highest potential with the edge value of the lattice, while in method B, we average all the conductors and the edge. After testing different configurations we found that, although both A and B introduce improvements, method B helps to reach equilibrium faster in more situations than A.

We tested both methods for setups with conductors of different sizes and for several potential values and ratios. Figure 4 shows one instance in which we use a similar configuration to the one in figure 1, but with much smaller conductors. Also, since the potentials used are 18, 12 and 6 V, we say that the configuration has a potential ratio of 3:2:1. Our aim is to track the required number of iterations to reach equilibrium, both near the center (asterisk) and near a corner (black dot), as depicted in figure 4(a). It is shown that method B is more efficient, meaning it converges in fewer iterations. Method B is even more efficient when used in configurations with larger potential ratios, such as 10:2:1. As we increase the size of the conductors, method A improved slightly, especially for low potential ratios, but method B is still preferable due to its wider range of effectiveness.

Finally, instead of assigning a constant value to all free points, we used an initial condition that was logarithmically decaying. This is because, at large enough distances, the infinite conductors simulated in our model can be approximated reasonably well as infinite

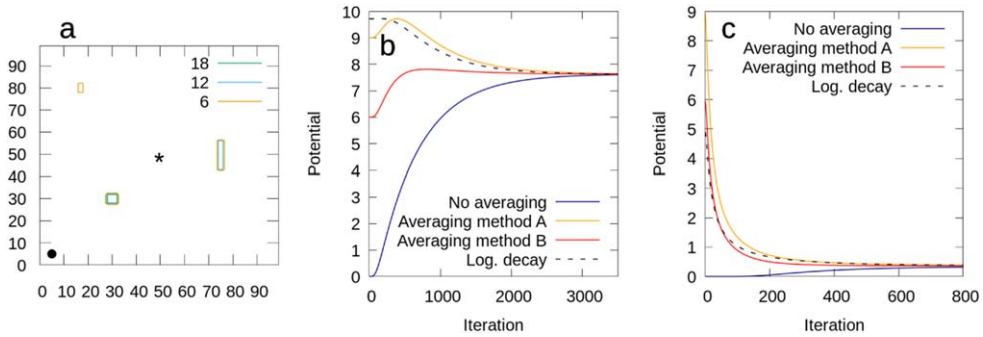

Figure 4. (a) Simulated configuration. Convergence of the asterisk and black dot are presented in (b) and (c) respectively.

wires. Therefore, to assign initial values, we measured the distance r_a between the free point and the center of one of the conductors, which we will call conductor a. From this, we could calculate an appropriate value [3] for the free point. This procedure was repeated for each conductor, so in the end the free point would be assigned a value of

$$\varphi_i = K_a \ln \frac{1}{r_a} + K_b \ln \frac{1}{r_b} + K_c \ln \frac{1}{r_c},$$

where the constants K_i contain information about the potential and location of the conductors and where this logarithmic decay intersects the plane. In this case, the intersection was chosen to be a circle with a diameter of twice the lattice size. Figure 4, shows how this method of setting initial values performs in comparison with method A and method B. In most of the configurations that we simulated, the logarithmic method was a close second. However, this has a positive side; it is always adequate. Whereas some situations are suited to either method A or method B, the logarithmic method is always good, if not optimal. Because of its versatility it is worthy of consideration, especially if one is looking to simulate a wide variety of conditions.

5. Error and computational cost

In order to determine the computational error introduced in the numerical solution φ_{relax}, we run the simulation with trivial boundary conditions, consisting of two uniform infinite wires with opposite charge, as can be seen in figure 5(a). This condition can be analytically solved to get the theoretical solution φ_{theo}. We take our reference potential to be the midpoint between the wires and set it to zero. In this setup, as we increase the distance from the wires, the potential decays towards zero. Therefore, we could also change our reference to infinity with no consequences. Now, we measure the absolute error as $e = |\varphi_{\text{relax}} - \varphi_{\text{theo}}|$. In order to analyze the behavior, we increase the lattice size and record the error.

In figure 5(a), P represents the point at which we measure the error. From electrostatic theory [3], the potential at P is given by

$$\varphi_{\text{theo}} = \frac{\lambda}{4\pi\epsilon_0} \ln \frac{(x+a)^2 + y^2}{(x-a)^2 + y^2}, \tag{10}$$

where x and y are the Cartesian coordinates of P relative to the center of the lattice, ε_0 is the permittivity of free space and a is half the distance between the wires. For simplicity, we set

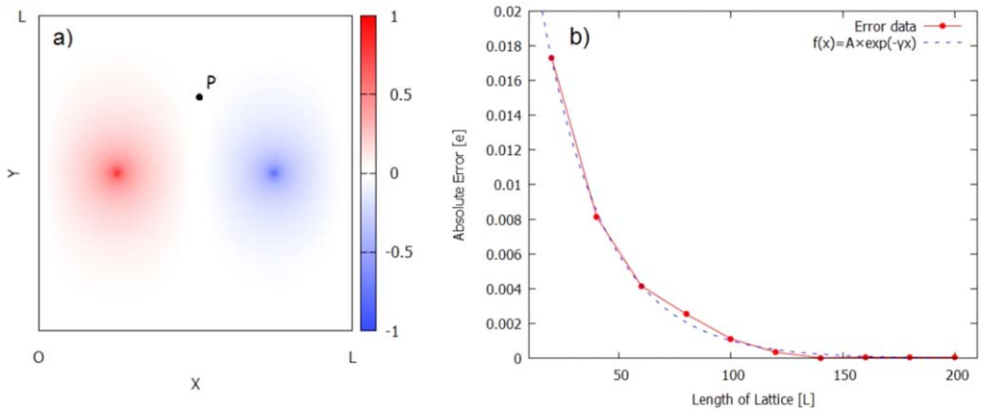

Figure 5. (a) Transverse section of two infinite wires, where L is the actual lattice side-length, and X,Y are the usual Cartesian coordinates. (b) Absolute error as a function of the lattice side-length. Error decreases exponentially, as can be seen in the fitting curve $f(x)$. We have $A = 3.48 \times 10^{-2}$ and $\gamma = 3.52 \times 10^{-2}$.

$\lambda/4\pi\ \epsilon_0 = 1$, reducing (11) to

$$\varphi_{\text{theo}} = \ln \frac{(x+a)^2 + y^2}{(x-a)^2 + y^2}. \tag{11}$$

In the numerical simulation, the reference is the edge of the lattice, as usual, which moves farther from the center, where the wires are located, as the lattice size increases. This causes the reference potentials of the simulation and the theoretical model to come closer to each other. These large lattice sizes reduce the effect of the edges, as can be seen in figure 5.

In contrast with the theoretical calculations, the reference potential in an experimental setup is usually much closer than infinity. For example, the conductors can be placed within a grounded boundary, which is exactly represented in our simulation[2]. Nonetheless, the comparison to the easy-to-solve, albeit fictitious, case of infinite wires shows that our confidence in the model is justified[3].

Another error source in the simulation relies on the criteria to stop the iterative process; the more iterations we do, the closer we approximate the real solution. However, it is clear that we cannot iterate infinitely—we must stop at some point. A suitable criterion for deciding when to stop the simulation is when every single free point changes by less than a certain specified tolerance. This affects not only the number of performed iterations, but the time the computer takes to output the solution.

As discussed above, the lattice size is a primary factor in the accuracy of the model, so we compared the convergence time and needed iterations before stopping the process for two precision uncertainties as a function of lattice side-length. The results are shown in figure 6.

The convergence time grows proportional to the square of the side-length, which is reasonable, since this is actually the area of the lattice. The number of iterations, however, tends to a plateau determined by the tolerance. Note how the required time increases sharply

[2] It might seem bizarre to attempt to bind, for example, a pair of infinite wires. However, potentials accurately modeled as conductors of infinite length can be easily obtained in a lab (for a concrete example, refer to section 6).
[3] The model is in fact better suited to these situations. Some theoretical models have issues when simulating because the reference potential is awkwardly placed. For example, a single infinite wire falls off proportional to $\ln(1/x)$, so its zero would have to be placed at a finite distance, implying a redefinition of the lattice edge.

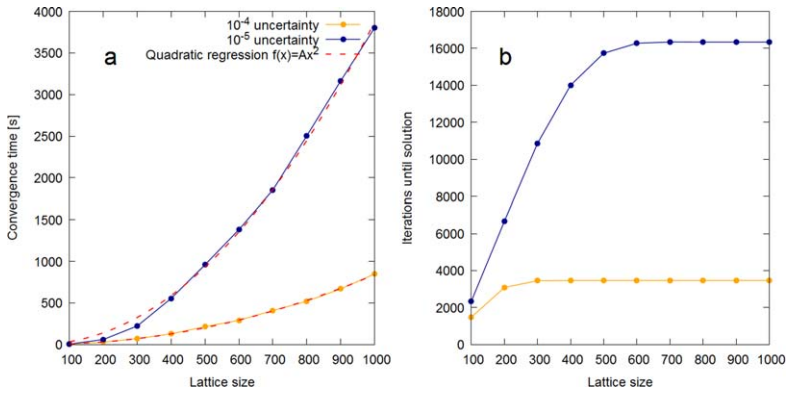

Figure 6. (a) Diagram of the needed convergence time for the system to relax with two different tolerance criteria, using 10^{-4} and 10^{-5} precision uncertainties. For the 10^{-4} uncertainty case we have $A = 5.976 \times 10^{-4}$, and for the 10^{-5} case $A = 2.638 \times 10^{-3}$. (b) is the number of iterations until the solution is reached.

with a reduction in tolerance, even in a single order of magnitude. While it is clear that for already low-precision uncertainties it gets increasingly difficult and impractical to keep improving the accuracy, we can get so close to the real solution in a short time (down to less than a few parts in ten thousand in about an hour), that it is unnecessary to do so.

The results were obtained running the simulation in a Linux machine (Ubuntu distribution), with a dual-core 1.9 GHz processor and 4 GB of RAM. The code was processed sequentially, as opposed to in parallel, in order to allow for direct comparison. It is noteworthy that the computing resources involved are relatively low, comparable with an average laptop of today, which highlights the accessibility of the relaxation method.

6. Experimental realization versus numerical model

To further prove the validity of our numerical model, we perform an experimental realization, which consists of measuring the potential around two charged metal plates, as presented in figure 7(a). A quintessential lecture example, the potential around the edges of parallel charged plates is commonly used to show how complicated the functional form of the potential can become, even for such a simple geometry. By comparing it with our numerical model, we hope, once more, to show its usefulness and simplicity. We submerged a rectangular piece of acrylic glass marked with a fine 2 mm grid in a water tray around 6 mm deep. There were two metal plates screwed onto the glass beforehand. After ensuring total water coverage of the glass and plates, we used jumper cables with crocodile tips to connect each plate to a Phywe DC universal power supply. Then, we set the power supply to 6 V, which in turn set the potential of the plates at 0 and 6 V. Finally, we used a Uni-T UT39C digital multimeter to measure the potential at different points of the grid. The negative terminal of the multimeter was connected to the negative terminal of the power supply, grounding it like the negative plate. On the other hand, the positive terminal was connected to a probe that was used to measure the potential at intervals of 4 mm in the submerged grid.

The obtained data from this experiment are shifted down so that the potential reference becomes the midpoint between the plates. Then, we normalize the data so the potential of the positive plate is 1 V. Finally, taking into account the size and position of the plates, we

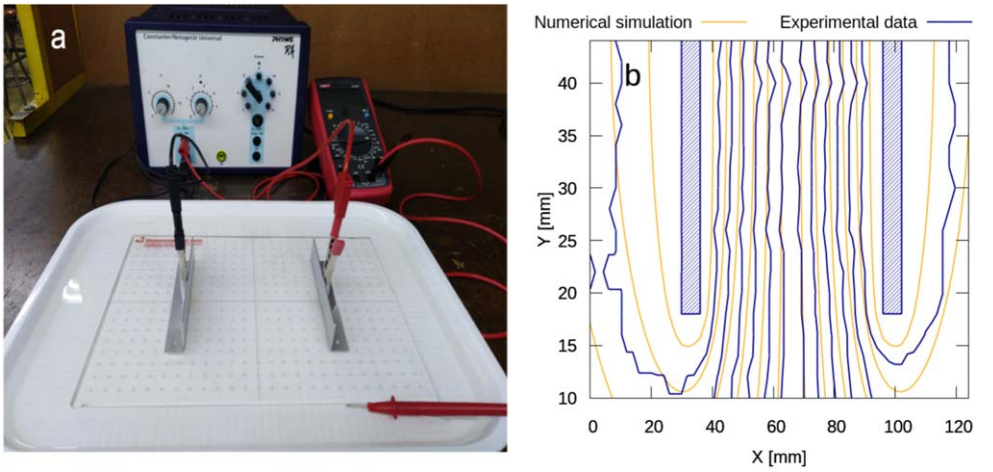

Figure 7. (a) Experimental setup with a 10 mm grid. (b) Experimental data compared with simulation.

simulated the system with our numerical model, using a large lattice of 1000×1000 to minimize the edge effects.

We can see from the results in figure 7(b) that the simulation agrees really well with the experiment, especially between the plates, and gets better as it approaches the middle of them, which in the graph corresponds to $Y = 46$. Moreover, we observe a remarkable approximation of the potential around the ends of the plates. Considering the great difficulty in theoretically calculating these edge effects, it becomes apparent that our numerical approximation is a very useful tool for modeling this phenomenon, not only for its fast results, but its accuracy.

7. Conclusions

In most cases, physical configurations do not allow for simple closed-form solutions, for example, the case of the two infinite parallel wires. In contrast, the relaxation method has excellent accuracy, versatility and simplicity, making it a powerful tool for the analysis of electrostatic systems. We demonstrated with examples the core principles of this method, and how it can be applied to specific problems in physics. Furthermore, this model can be optimized, and adapted for a wide range of systems (see [1] and [2]). This, coupled with the easy access to the needed resources, makes the relaxation method and its applications an excellent topic to introduce numerical methods for solving physical problems. Its advantages, limitations, accuracy and uncertainties, exemplify commonly encountered areas of importance when doing computational physics. Its analysis, as carried out in this article, provides valuable insight, and a starting point for students who desire to learn more about these ways of solving problems.

ORCID iDs

Felipe Reyes-Osorio https://orcid.org/0000-0002-6399-2524
Juan Manuel Scarpetta-Ramirez https://orcid.org/0000-0002-4604-3394

Karen Rodriguez-Ramirez https://orcid.org/0000-0003-2860-9208

References

[1] Abdallah S and Dreyer J 1988 Dirichlet and Neumann boundary conditions for the pressure Poisson equation of incompressible flow *Int. J. Numer. Meth. Fl.* **8** 1029–36
[2] Goldstraw E E *et al* 2018 Comparison of methods for modelling coronal magnetic fields *Astron. Astrophys.* **610** A48
[3] Purcell E M 1985 *Electricity and Magnetism (Berkeley Physics Course)* vol 2 (New York: McGraw-Hill)
[4] Maver W 1918 *Electricity, its History and Progress. The Encyclopedia Americana.* vol 10 (New York: Encyclopedia Americana Corp.) pp 174–6
[5] Cannell D M 1999 George Green: an enigmatic mathematician *Am. Math. Month.* **106** 136–51
[6] Rouse Ball W W 2010 *A Short Account of the History of Mathematics* (Urbana, IL: Project Gutenberg) pp 339–42
[7] Olver P J 2016 *Introduction to Partial Differential Equations* (Berlin: Springer) pp 152–60
[8] Bak J and Newman D J 2007 *Complex Analysis* (Berlin: Springer) pp 226–7
[9] Freitag E and Busam R 2009 *Complex Analysis* (Berlin: Springer) p 93
[10] Southwell R V 1946 *Relaxation Methods in Theoretical Physics* (Oxford: Oxford University Press) pp 19–21
[11] Sadiku M N O 2001 *Numerical Techniques in Electromagnetics* (Boca Raton, FL: CRC Press) pp 147–52
[12] Rüter R *et al* Hyperbolic relaxation method for elliptic equations *Phys. Rev.* D **98** 084044
[13] Papamichael N and Symm G T 1975 Numerical techniques for two-dimensional Laplacian problems *Comput. Method. App.* M **6** 175–94
[14] Goffin J L 1980 The relaxation method for solving systems of linear inequalities *Math. Oper. Res.* **5** 388–414
[15] Troyer M 2006 *Computational Physics* (Zürich: ETH Zürich) p 22